Journal of Polymer Research (2020) 27: 293
https://doi.org/10.1007/s10965-020-02266-3

ORIGINAL PAPER

Low band gap polymers based on the electrochemical polymerization of Phenazine: studies on the color changing ability in near-infrared region

Rena Simayi[1] · Aray Murat[2] · Mukhtar Imerhasan[1] · Maxhur Mijit[2] · Mamtimin Mahmut[1]

Received: 23 May 2020 / Accepted: 18 August 2020 / Published online: 4 September 2020

Abstract

In this work, two quinoxline type monomers, 10,14-bis(4-octyl-2-thienyl)-dipyrido[3,2-*a*:2′,3′-*c*] [1, 2, 5] thiadiazolo[3,4-*i*] quinoxaline (OTPTP) and 10,14-bis(4-octyl-2-thienyl)-dibenzo[*a, c*][1,2,5]thiadiazolo [3,4-*i*] quinoxaline (OTBTP) were prepared, and the electrochromic features of their polymer films that were synthesized on the ITO glass surface by electrochemical polymerization were studied. The electronic characteristics of two different electron-withdrawing groups and their influences on the electrochemical polymerization of monomers and electrochromic performance of the obtained polymers were observed. The electronic performance of monomers illustrated that OTBTP can be polymerized in the lower potential range than OTPTP due to the stronger electron-withdrawing capability of the electron-withdrawing groups in OTPTP which contains two dipyridine units. The UV Visible NIR spectra analysis showed that both polymers, POTPTP and POTBTP, have one broad absorbance band in the region of 400 ~ 1600 nm at the neutral state. The electrochromic analysis revealed that the two polymer films exhibited reasonable optical contrasts in the infrared region of 1000 ~ 1600 nm with low response time (about 5 s) and low band gap.

Keywords [1,2,5]thiadiazolo[3,4,i] quinoxaline · Donor-acceptor · Electrochemical polymerization · Low band gap polymer · Electrochromic properties

Introduction

Electrochromic devices can reversibly change their color and transmittance when different potential are applied to the electrochromic material and cause their redox reactions [1]. There are two types of electrochromic materials categorized in accordance with the difference in chemical structure. The first class of electrochromic materials is the inorganic materials [2], such as WO_3, NiO_2 and TiO_2, which are used as excellent materials in optical shutters and smart windows. Organic materials with electrochromic properties including organic dyes and conjugated polymers are the second type of electrochromic materials. Polymer-based electrochromic devices have many advantages over inorganic electrochromic devices, such as flexibility, higher coloration efficiency, and faster switching [3]. More importantly the electrochromic performance of the devices can be adjusted by the molecular structure modification of the conjugated polymers. Hence, the polymer-based electrochromic devices can be used as smart windows [4] and paper-like displays [5]. Especially those electrochromic devices which use organic molecules with near-infrared (NIR) absorption ability have many potential applications, including security inks, optical and electronic biosensors [6, 7], bioimaging [8], and anticancer and antimicrobial therapies [9]. The electrochemical polymerization of suitable monomers that possessing suitable redox activity may produce promising low band-gap conjugated polymers which can be the most promising materials for electrochromic materials in NIR region [10, 11]. In the electrochemical mechanism of conjugated polymers, a neutral monomer unit can be attacked or couple with a radical cation. In the oxidized states of conjugated polymers, the counter anions are ‘doped’ into

✉ Mamtimin Mahmut
subhijan@xju.edu.cn

[1] Key Laboratory of Energy Materials Chemistry, Ministry of Education; Key Laboratory of Advanced Functional Materials, Autonomous Region, Institute of Applied Chemistry, Urumqi Key Laboratory of Green Catalysis and Synthesis Technology, College of Chemistry, Xinjiang University, Urumqi 830046, Xinjiang, People’s Republic of China

[2] School of Chemical Engineering and Technology, Xinjiang University, Urumqi, China

the conjugated polymers and the polymers exhibit a delocalized p-electron band structure. The optical performances, especially the absorption characteristics of the conjugated polymers in the near infrared region, are greatly affected by the width of the band gap between valence band and conduction band [12–14].

The quinoxaline structure has been wildly used as the electron-withdrawing group in the preparation of low-band gap electrochromic polymers and the literature results showed that this type of conjugated polymers with low-band gap performed favorable electrochromic capability [15–21]. Thus in our work, the quinoxaline units which contain larger planar conjugation were used as the acceptor unit to prepare NIR absorbing polymers [22–24]. Our research results show that the polymers synthesized by electrochemical polymerization using quinoxaline type monomers with larger planar conjugation exhibit low-band gap characteristics and good NIR absorption ability in the region 800 ~ 1600 nm. The results also indicate that a larger planar conjugation, more heteroatom in quinoxaline structure, and stronger electron withdrawing ability improves the electrochromic ability and NIR absorption ability in the 800 ~ 1600 nm region. It is also reported elsewhere that modifying the position and the type of heteroatom in the acceptor group is a useful method to control the electron-withdrawing abilities of electron acceptor groups and eventually enabling the easier intramolecular electron transfer in the design of conjugated polymers with low-band gap [25]. Therefore, in this study two quinoxaline type monomers, 10,14-bis(4-octyl-2-thienyl)-dipyrido[3,2-*a*:2′,3′-*c*] [1, 2, 5] thiadiazolo[3,4-*i*] quinoxaline (OTPTP) and 10,14-bis(4-octyl-2-thienyl)-dibenzo[*a, c*-][1,2,5]thiadiazolo [3,4-*i*] quinoxaline (OTBTP), were prepared. Two polymer films with low-band gap (Chart.1) and good electrochromic behavior and excellent absorption ability in the NIR region were synthesized onto ITO glass surface by the electrochemical polymerization of these two monomers. The electrochromic properties, switching properties and NIR absorption abilities of these polymers were then investigated. The influence of planar conjugation and the N atom in electron acceptor unit on the electrochemical and electrochromic features of the polymers were also explored.

Experimental

Materials

All the chemicals needed for the experiments in this paper were provided by Shanghai Boka Chemical Co., and employed as purchased except separately indicated. 1,10-phenanthroline-5,6-dione (1) [26], 4,7-dibromo-5,6-dinitrobenzo[1,2,5]thiadiazole (3) [27] were prepared following a known method that reported elsewhere. The tetrahydrofuran (THF) that was used in the experiment was prepared by distilling over sodium using benzophenone as an indicator. In electrochemical polymerization and electrochemical performance studies, tetra-n-butylammonium hexafluorophosphate (TBAPF6) was used as the electrolyte, and a mixed solvent comprising of dichloromethane (DCM) and acetonitrile (ACN) (95/5, v / v) was employed as the solvent.

Apparatus

A VARIAN INOVA-400 spectrometer (400 MHz) was used to record the ^{1}H-NMR spectrum of the intermediate with $CDCl_3$ as the solvent. The electrochemical polymerization and electrochemical performances were examined using a Zahner-Zennuim electrochemical workstation as a working platform. Electrochemical polymerization was carried out in a device which was consisted of the counter electrode (a platinum sheet), the reference electrode (a silver wire) and the working electrode (a conductive ITO glass). Shimadzu UV-3600 was used to record the spectrum of the polymer film, and Shimadzu UV-3600 and MCP-1 regulator were connected to test the electrochromic properties of the polymer film.

Experimental procedures

The intermediates and polymers were synthesized according to the synthetic routs are shown in Scheme 1.

Synthesis of tributyl(4-octylthiophen-2-yl)stannane(2) [28]

Tributyl(4-octylthiophen-2-yl)stannane was prepared using a modified procedure. 4-octylthiophen (39.3 g, 40 ml, 200.0 mmol) dissolved in freshly distilled tetrahydrofuran (250 ml) was cooled down to −100 °C and maintained for 30 min. *n*-BuLi solution (2.5 M in hexane, 80 ml, 200.0 mmol) was syringed into the reaction, during which time the temperature maintained under −100 °C. After completion the temperature was maintained at −78 °C for another 2 h. Then the contents were warmed up to room temperature by keeping the reaction mixture in a cooling bath during warming up, and was left to stir for 2 h. The reaction temperature was then lowered again to −100 °C and tributyl chloride (200.0 mmol, 60 ml) was added. The temperature was then raised up to −78 °C and stirred at this temperature for 1 h, before naturally warming up to room temperature and left to react overnight. After washing with saturated sodium bicarbonate solution, the resultant mixture was extracted with petroleum ether, dried over $MgSO_4$, filtered and solvent evaporated under reduced pressure. A Kugelrohr distillation was then performed to obtain the final product as a light-yellow oil (yield 98%). ^{1}H NMR (400 MHz, $CDCl_3$) δ: 7.18(d, J = 2.8 Hz, 1H); 6.96(d, J = 1.2 Hz, 1H); 2.66 ~ 2.62(t, 2H); 1.61 ~ 1.52(m, 8H); 1.42 ~ 1.28(m, 16 h); 1.11 ~ 1.06(m, 6H); 0.92 ~ 0.86(m, 12H).

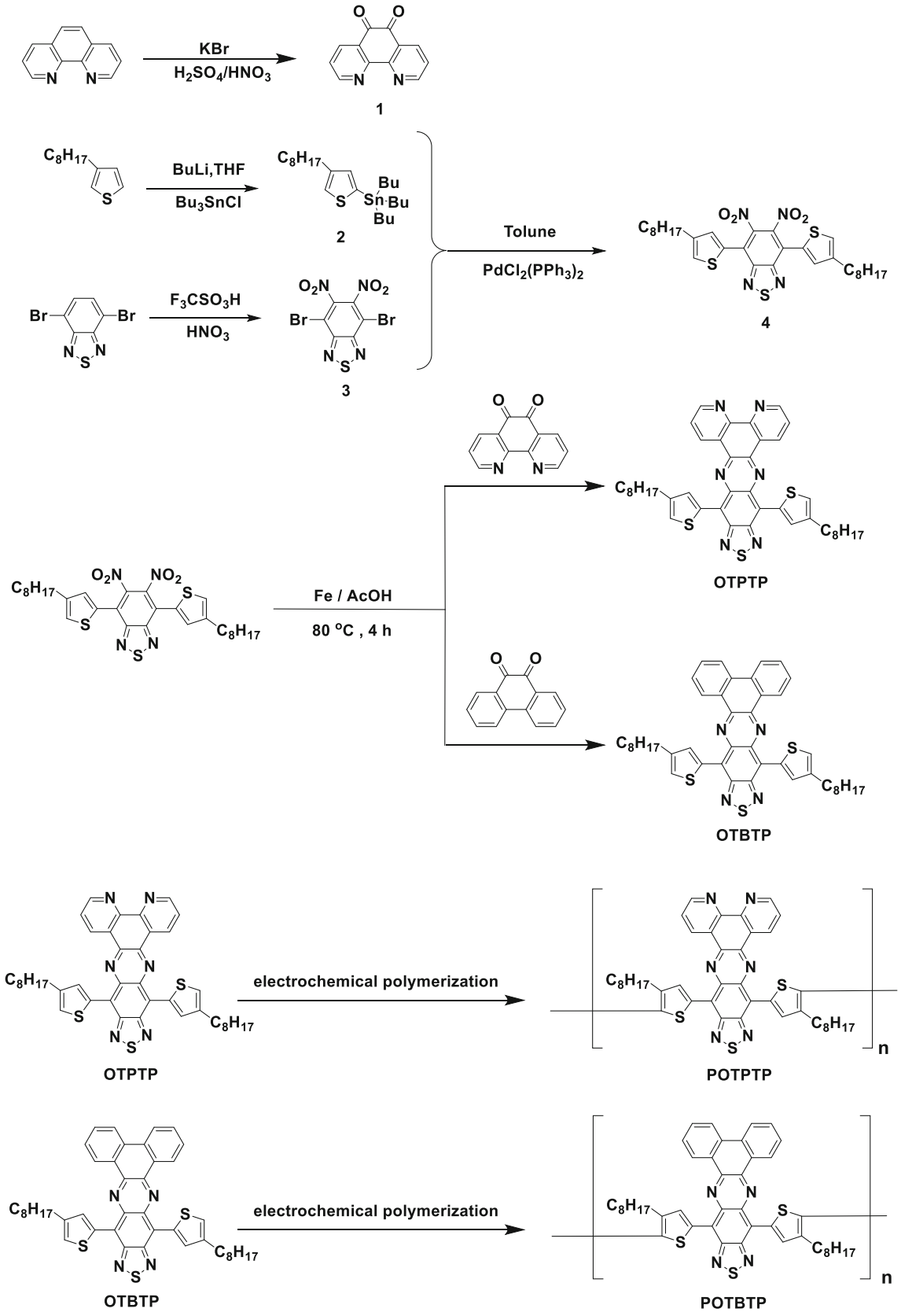

Scheme 1 Schematic route for the synthesis of monomers and polymers

Synthesis of 4,7-bis(4-octylthiophene-2-yl) -5,6-dinitro-[1,2,5]benzothiadiazole(4) [29]

4,7-bis(4-octylthiophene-2-yl) -5,6-dinitro-[1,2,5]benzothiadiazole was prepared by a modified procedure. To a 120 ml Schlenk tube, 4,7-dibromo-5,6-dinitro-2,1,3-Benzothiadiazole (2.91 g, 10.0 mmol), $Pd(PPh_3)_2Cl_2$ (0.14 g, 0.2 mmol) and tributyl(4-octylthiophen-2-yl)stannane (10.60 g, 22.0 mmol) were added. The reaction flask was evacuated and back filled with argon. Anhydrous THF (60 ml) was syringed into the Schlenk tube and the reaction mixture heated to reflux for 2 days. The resultant mixture was cooled to room temperature and the solvent was evaporated to give a deep red oil, which was then dissolved in ethanol with heating and subsequently cooled in refrigerator for overnight. Needle like orange red solid was obtained after filtration and was purified by column chromatography (silica gel, petroleum ether: dichloromethane = 3: 1) to obtain an orange solid (91%). ^{1}H NMR (400 MHz, $CDCl_3$) δ: 7.32 (d, J = 2.8 Hz, 4H); 2.67 (t, 4H); 1.66 ~ 1.61 (m, 4H); 1.35 ~ 1.28 (m, 20H); 0.90 ~ 0.86 (m, 6H).

Synthesis of 10,14-bis(4-octyl-2-thienyl)-dipyrido[3,2-*a*:2′,3′-*c*][1,2,5]thiadiazolo[3,4-*i*]quinoxaline (OTPTP) [30, 31]

At 80 °C, the reduction reaction of the intermediate 4 (1228 mg, 2 mmol) with iron powder (1200 mg, 20 mmol) as the reducing agent was carried out for 4 h in acetic acid (100 ml). After the reaction was completed, the contents were poured into distilled water and were extracted using DCM followed by drying with $MgSO_4$. After the solvent was evaporated, acetic acid (50 ml) and 1,10-phenanthroline-5,6-dione (231 mg, 1.1 mmol) were added into the reaction flask and left to react at room temperature with stirring for 48 h, before deionized water was added to the resultant mixture. After extraction with $CHCl_3$, the organic phase was washed with aqueous sodium carbonate and brine and dried with $MgSO_4$ followed by the remove of solvent under reduced pressure. Column chromatography (silica gel, $CHCl_3$:CH_3OH = 20:1) was used to obtain the desired product after using $CHCl_3$ as the eluent to wash out the impurities. After the solvent was evaporated, the product was dried under vacuum at 60 °C for 48 h resulting in a deep blue crystal (529 mg, 73%). ^{1}H NMR (400 MHz, $CDCl_3$) δ: 8.97 (s, 2H); 8.87 (s, 2H); 8.48 (s, 2H); 7.27 ~ 7.25 (m,2H); 6.93 (s, 2H);2.62 (s, 4H); 1.72 (s, 4H); 1.45 ~ 1.25 (m, 20H); 0.94 ~ 0.90 (m, 6H).

Synthesis of 10,14-bis(4-octyl-2-thienyl)-dibenzo[*a*, *c*][1,2,5]thiadiazolo[3,4-*i*]quinoxaline (OTBTP)

The synthesis of the monomer followed a procedure similar to the synthesis of OTPTP, through the reaction of compound 4 and 9,10-phenanthrenequinone. Column chromatography (silica gel, $CHCl_3$: petroleum ether (60 ~ 90) =1:1) was then employed to obtain the final product as a green solid (85%). ^{1}H NMR (400 MHz, $CDCl_3$) δ: 9.10 (d, J = 7.6 Hz, 2H), 8.65 (s, 2H), 8.17 (d, J = 8.0 Hz, 2H), 7.57 ~ 7.46 (m, 4H), 7.17 (s, 2H), 2.71 ~ 2.67 (m, 4H), 1.77 ~ 1.72 (m, 4H), 1.48 ~ 1.25 (m, 20H), 0.94 ~ 0.90 (m, 6H).

Results and discussion

UV-Vis-NIR spectrum of monomers

Figure 1 is the UV-Vis-NIR absorption spectrum of quinoxaline monomers'(OTPTP and OTBTP) solution (c = 3.66×10^{-5} mol/L) in $CHCl_3$. It can be seen from the UV-Vis-NIR spectrum that the monomer OTPTP has two wide absorption bands in the range of 300–1000 nm. These two absorption bands are caused by the π-π* transition of the molecular orbital, and the maximum absorption peaks appear respectively at 341 nm and 714 nm. The monomer OTBTP has three absorption bands in the range of 300–850 nm, and the maximum absorption peaks appeared at 337 nm, 420 nm, and 681 nm, respectively. Comparing with the corresponding absorption peaks of OTBTP, the two absorption peaks of the monomer OTPTP has red shifts about 4 nm and 33 nm, respectively. It can be clearly observed from the spectra that the absorption band of OTPTP around 550 nm ~ 900 nm is wider than the absorption band of OTBTP. The red shift of the absorption peaks of the quinoxaline monomer and the broadening of the absorption peaks are due to the difference in the structure of the electron-deficient groups of the quinoxaline monomer [23, 24]. In the electron-deficient group of OTPTP, there exists two pyridine moieties which would lead to a

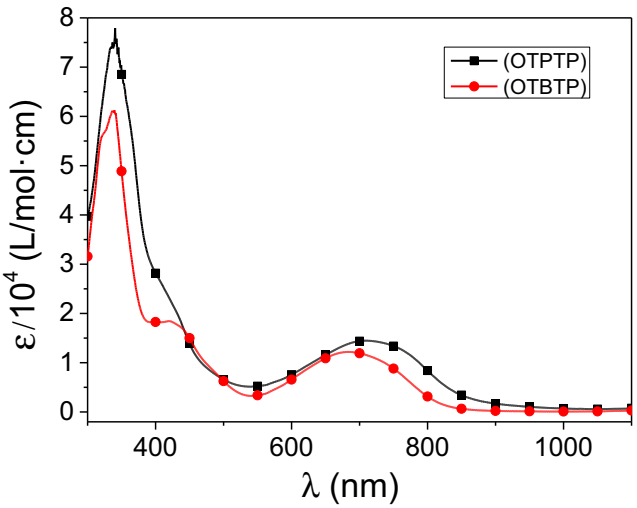

Fig. 1 UV-vis spectra of OTPTP and OTBTP in DCM (The concentration of monomers is c = 1×10^{-6} mol/L)

greater electron-deficiency of quinoxaline units and a greater degree of conjugations of OTPTP. Therefore, the changes in structure is reflected in the difference of the electrochemical and optical properties of the two quinoxaline type compounds.

Electrochemistry

In the electrochemical polymerization, $TBAPF_6$ was used as the electrolyte for all the electrochemical studies in this work [22–24]. When the electrochemical polymerization was carried out, the electrolyte concentration was 0.1 M, and the quinoxaline monomers concentration was 0.01 M. In the following studies of electrochemical properties, the electrolyte concentration was still 0.1 M, and the CV was carried at a scan rate of 100 mV.

The solution of monomer OTPTP was scanned from 0 to 1.3 V with the results presented in Fig. 2a. It can be clearly seen from the curve that OTPTP has a pair of redox peaks appearing at 1.18 V and 0.9 V, respectively. Therefore, at first, the electrochemical polymerization of OTPTP was carried out in the range of 0 to 1.3 V. However, it was found that the electrochemical polymerization scanning curve was very irregular, and the polymer was not uniformly deposited on the ITO surface and agglomeration occurred. This phenomenon may be due to the presence of the dipyridine ring in the electron-deficient unit of OTPTP thus enhancing the electron-withdrawing ability of the electron-deficient unit and reducing the density of electron clouds on the thiophene ring linked to quinoxaline. When the oxidation potential exceeded 1.18 V, more OTPTP was oxidized on the surface of the ITO electrode, and the polymerization reaction proceeded violently thus a regular polymer film cannot be obtained. To prepare a uniformly distributed polymer film, the electrochemical polymerization potential range was adjusted in the subsequent electrochemical polymerization. When polymerization was performed in the range of 0 to 1.1 V, a relatively regular polymer film is obtained. When the electrochemical polymerization potential was further adjusted to 0.4 to 1.1 V, the distribution of the polymer film was even better, and the reproducibility of the polymerization reaction was exceptionally good. As the electrochemical polymerization proceeds, the thin polymer film was deposited on the ITO surface and two new oxidation potentials were occurred at +0.65 V and + 0.91 V. As the polymer film became thicker, these two oxidation potentials increased to +0.77 V and + 1.09 V, respectively (Fig. 2c). During the

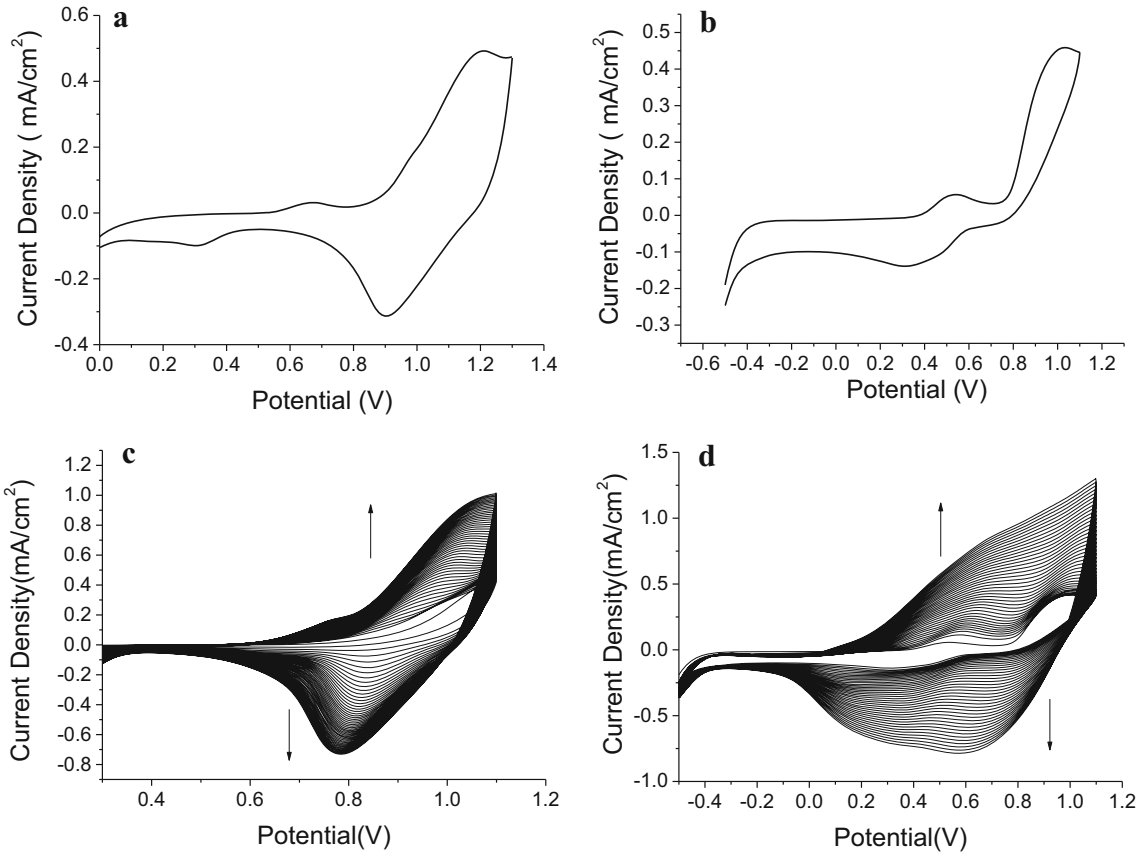

Fig. 2 Single scan cyclic voltammograms of (**a**) OTPTP and (**b**) OTBTP at 100 mV/s in ACN/DCM (5:95) solution containing 0.1 mol/L $TBAPF_6$ on ITO electrode; Repeated potential scan electrochemical polymerization of(**c**) OTPTP and (**d**) OTBTP in the same solvent-electrolyte system

polymerization reaction, the reduction potential of POTPTP appeared at +0.83 V and eventually reached to +0.77 V.

The above synthesis method was used in the electrochemical polymerization process of OTBTP. In Fig. 2b, the solution of monomer OTBTP was scanned from −0.5 V to +1.1 V. As the electrochemical polymerization proceeds, two new oxidation peaks were occurred at +0.55 V and + 1.0 V. As the polymer film became thicker, followed by the increase of the oxidation peaks, the first oxidation peak eventually disappeared (Fig. 2d). It is also observed that the reduction peak of POTBTP increased, and the reduction wave at +0.75 decreased to +0.57 V, in contrast.

The change of redox potential in the electrochemical polymerization process is due to the coverage of ITO glass electrode surface with polymer film formed by electrochemical polymerization, thus the thiophene structure in monomer quinoxaline became less susceptible to oxidation on the electrode. In addition, it can be seen from Fig. 2c and Fig. 2d that the oxidation potentials of the monomer OTBTP were lower than that of the monomer OTPTP. The lower oxidation potential indicates that OTBTP is easier to be oxidized, because the electron-deficient unit in OTBTP has a lower electron-withdrawing ability than OTPTP, making the electron density of thiophene ring in OTBTP structure higher and thus being more susceptible to oxidization [17]. In addition, the HOMO energy level of the monomer OTBTP was higher than that of OTPTP [32].

The results of the scan rate dependence of polymer POTPTP and POTBTP were shown in Fig. 3. The test results show that there is a good linear relationship between the peak current and the scan rate at different scan rates. The polymer exhibits good electrochemical stability at different scan rates. Even at high scan rates, the polymer film has good reversible redox capabilities. Figure 3a shows that one anodic current is clearly observed at +0.7 V in the scan rate dependence curve of POTPTP. The anodic current at +1.2 V can be seen at the scan rate of 100 mV/s and 150 mV/s, but disappeared when the scan rate was higher than 150 mV/s. Therefore, +1.3 V was chosen as the upper limit value of the electrochemical scanning range. The scan rate dependence results of POTBTP showed that the anodic current of about +0.9 V can be fully observed at any scan rate (Fig. 3c), indicating that +1.0 V can be chosen as the highest potential for electrochemical polymerization of POTBTP. However, the

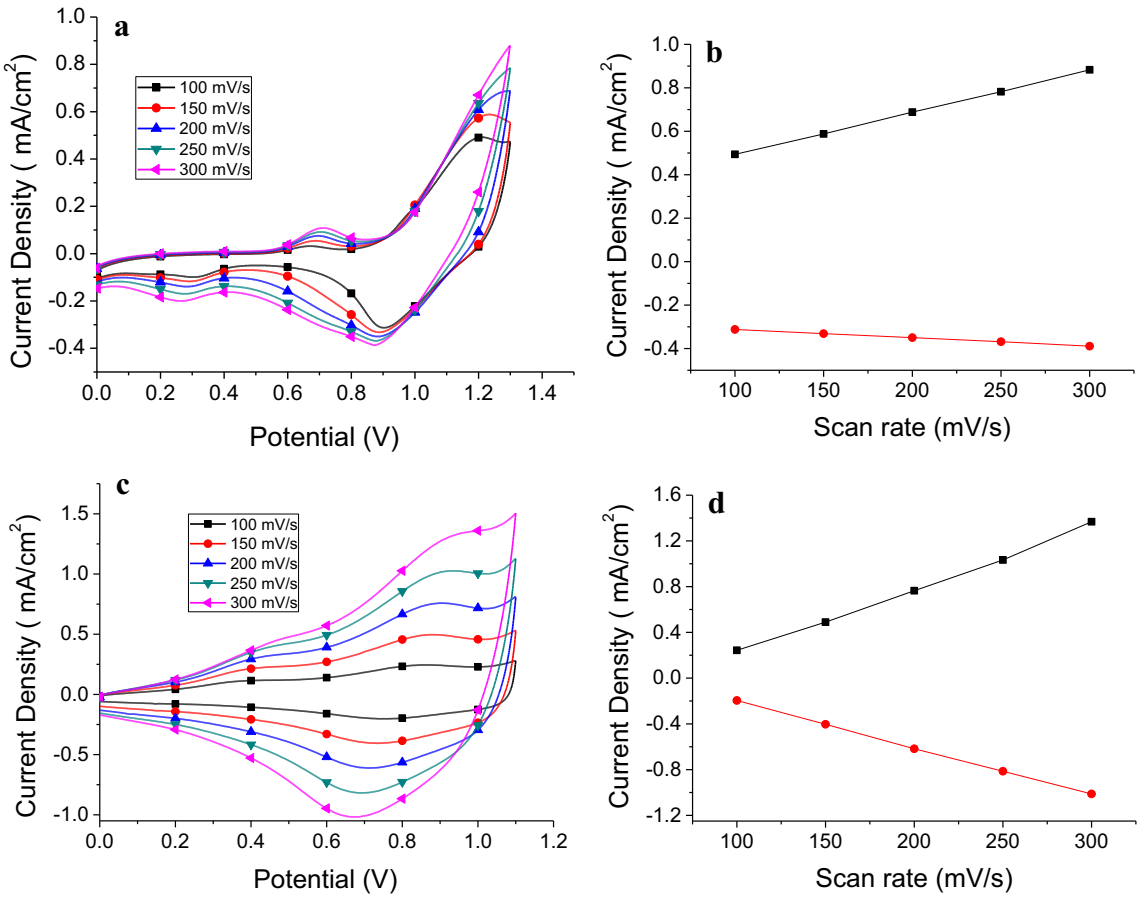

Fig. 3 Scan rate dependence of (**a**) POTPTP film and (**c**) POTBTP in monomer free ACN/DCM (95:5) solution containing 0.1 mol/L $TBAPF_6$; Relationship of anodic (black square) and cathodic (red circled) current peaks as a function of scan rate for (**b**) POTPTP and (**d**) POTBTP films

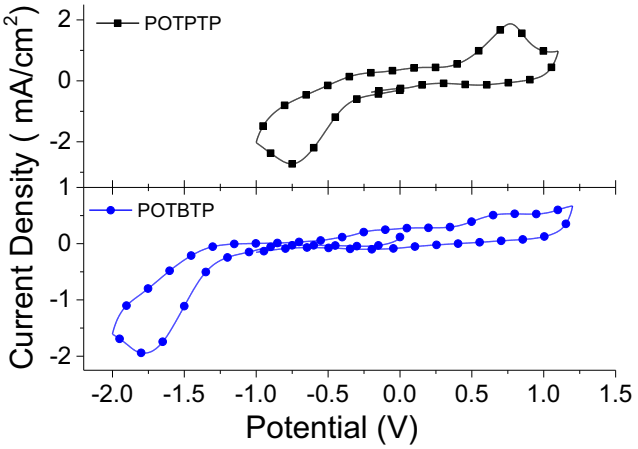

Fig. 4 Cyclic voltammogram of POTPTP and POTBTP films in 0.1 mol/L $TBAPF_6$/ACN/DCM (5/95, *V*/V) at scan rate of 100 mV/s

electrochemical polymerization results showed that a fully qualified polymer film on ITO glass electrode surface cannot be obtained at this current, thus +1.1 V was chosen as the highest potential for electrochemical polymerization of POTBTP.

The p-type and n-type doping performance results of the two polymers are shown in Fig. 4. It can be seen from the test results that the p-type doping of POTPTP happened at +0.76 V, while the n-type doping occurred at −0.75 V. POTBTP had two p-type doping at +0.09 V and + 0.69 V, while the corresponding n-type doping occurred at −0.10 V and − 1.76 V, respectively. According to the method reported in the literature, the HOMO-LUMO value of the two polymers can be calculated based on the UV-Vis-NIR spectrum and the results obtained by electrochemical studies, and summarized in Table 1 [33]. From the results in Fig. 4, it can be concluded that comparing to the POTBTP films, the p-doping of the POTPTP films is more difficult while the n-doping happens to be easier due to the difference of the nature of the electron-deficient units in the two polymers and this was fully discussed above.

Electrochromic studies of polymers

After selecting the best monomer concentration, electrolyte and polymerization voltage range based on the electrochemical polymerization performance research, the two polymers, POTPTP and POTBTP, were fixed onto ITO glass surface, and the polymer film was immersed in phenylhydrazine for 5 h. The polymer recovers from the doped state, which was achieved during the electrochemical polymerization, to the neutral state. Then the UV-vis-NIR spectra were taken (Fig. 5), and the results revealed that the two polymers showed similar absorption bands around 600–1600 nm (λ_{max} = 995 nm for POTPTP and λ_{max} = 1011 nm for POTBTP). These wide band absorption peaks can be attributed to three aspects. Firstly, during the oxidation and reduction in electrochemical polymerization process, the quinoxaline unit in the polymer structure possesses a strong electron withdrawing ability and exhibits electron deficiency, while the thiophene ring has a strong electron donor characteristic thus presenting electron enrichment. This makes the thiophene ring in the polymer structure susceptible to doping during the electrochemical oxidation process. As the polymer film becomes thicker, the dedoping of the doped ions that were implanted into the polymer film became slow. Hence, in the electrochemical polymerization, part of the doped ions are trapped in the polymer film. Therefore, the two polymer films cannot be completely restored to the neutral state during the dedoping process of phenylhydrazine treatment [32]. The experimental phenomenon that the electrochemically polymerized film cannot be restored to the neutral state and the doped ions are trapped in the internal structure of the polymer film was reported elsewhere [18, 22–24, 27, 34], and was also supported by the CV research results in this article (which was discussed above, see Fig. 2). Secondly, during the electrochemical polymerization process, agglomeration occurs between the polymer molecules, thereby increasing the conjugation between them, and subsequently causing the red-shift and widening of the absorption peak. Thirdly, the broad absorption band of the two polymers in the near infrared area was caused by the intramolecular electron transfer which was caused by the transfer of electrons from the electron-rich thiophene ring to the electron-deficient quinoxaline unit in the polymer structure [22–24, 28]. It can also be known from the spectral data of the two polymers that the maximum absorption peak of the polymer POTBTP film was red shifted by 16 nm compared with the absorption band of the polymer POTPTP film. From the perspective of molecular structure, the absorption band of POTPTP is expected to appear at a longer wavelength than that of POTBTP. However, the experiments exhibited the opposite results shown in Fig. 5

Table 1 Summary of electrochemical and optical properties of polymer films on ITO glass

	E_{mon}^{ox}/ V	$E_{p\text{-}doping}$/ V	$E_{p\text{-}dedoping}$/ V	$E_{n\text{-}doping}$/ V	HOMO/ eV	LUMO/ eV	λ_{max}/ nm	E_g^{op}/eV	E_g^{ec}/eV
POTPTP	0.8	0.76	0.55	−0.75	−5.13	−4.44	995	0.79	0.69
POTBTP	0.3	0.09, 0.69	−0.10	−1.76	−4.23	−3.51	1011	0.79	0.72

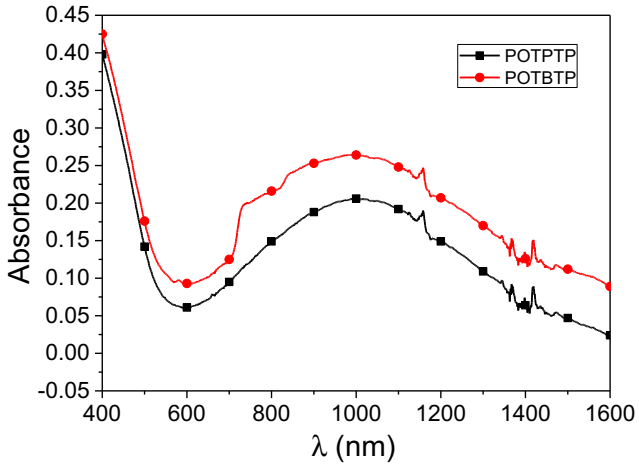

Fig. 5 UV-vis-NIR spectra of POTPTP and POTBTP at neutral state

and Fig. 8. This is due to the easy doping and considerably difficult dedoping of POTBTP comparing to POTPTP. The electrochemical polymerization results of POTPTP and POTBTP (Fig. 2) and electrochemical properties of these two polymers (Fig. 3) also support this view.

Scanning electron micrographs (SEM) were used to investigate the morphologies, which are related to the spectroelectrochemical properties, of the POTPTP and POTBTP films on ITO glass. As shown in Fig. 6, the morphology of the POTPTP film shows tight smooth surface and has few small clusters (Fig. 6c) while POTBTP film shows big clusters with continuous channels (Fig. 6d), which may be a benefit for the movement of the doping ion and improving color conversion ability [35].

The X-ray diffraction (XRD) spectra for the two polymer films on ITO glass were then obtained, which are presented in Fig. 7. The characteristic peaks of ITO glass at 2θ of 21.57°, 30.49°, 35.50°, 50.77° and 60.46° are observed in the two spectra, corresponding to the (211), (222), (400), (440), and (622) crystal faces of In_2O_3 on the surface of ITO glass [36]. The X-ray diffraction spectra of POTPTP and POTBTP films each showed two broad diffraction peaks. For the POTPTP film, these two broad peaks appeared approximately at 2θ of 5° ~ 14.76° and 14.76° ~ 39.68° in the XRD spectrum. In the case of the POTPTP film, they appeared at 2θ of 5° ~ 10.10° and 10.10° ~ 39.46°. The diffraction peaks in low angle range are generally correlated with the inter-chain spacing of the polymer chains and the diffraction peaks in high angle range are corresponding to the (020) reflection of the polymer backbone which are related to intermolecular π–π* stacking [37].

A UV-Vis-NIR spectrometer and a potentiostat were connected to investigate the discoloration ability of the two polymer films at different potentials (Fig. 8). The color change of the polymer POTPTP film in the neutral state and the oxidized state was tested between +0.6 V and + 1.3 V, namely p-doping and dedoping. The color change of the polymer POTBTP film between the neutral state and the oxidized state was tested between 0 V and + 1.1 V.

The electrochromic results of the polymer POTPTP film was shown in Fig. 8a. The polymer POTPTP film was yellow-green in the neutral state, and there was a wide absorption band between 600 nm and 1600 nm in the visible-near infrared region. When the applied potential gradually increased from +0.6 V to higher potential, the color of the polymer film faded, gradually changing from yellow-green to gray. In contrast, gradually lowering the potential from a high potential to +0.6 V caused the darkening of the color of the film, returning to a yellow-green color. This color change process showed

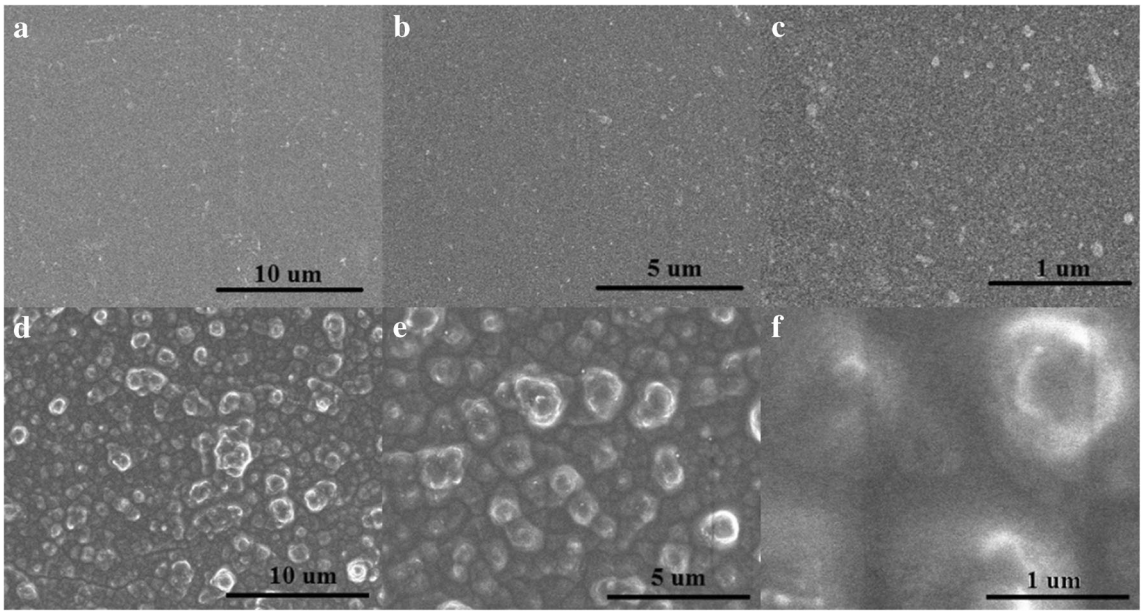

Fig. 6 SEM images of (**a**) ~ (**c**) POTPTP film, (**d**) ~ (**f**) POTBTP film

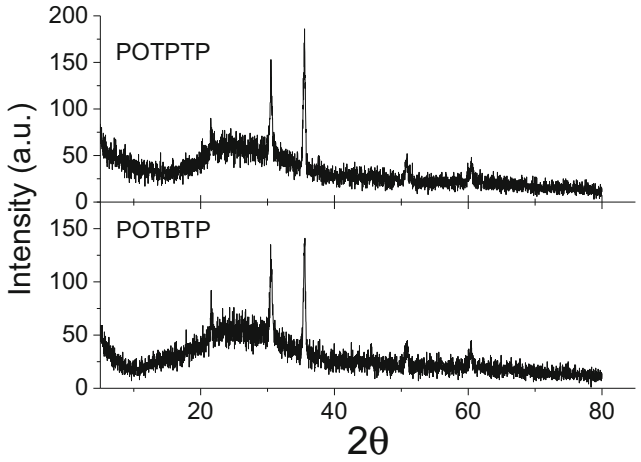

Fig. 7 XRD patterns of the polymer films

that the polymer was more prone to π-π * transition as the p-doping degree increases. As the oxidation potential increases from +0.6 V to +1.3 V, the absorption peak at 995 nm of the polymer film red-shifted, with a red shifting value about 376 nm, and eventually appeared at 1294 nm. As the applied potential increases, the absorption peaks of the polymer film further red-shifted. This is because as the applied potential increases, the electron-deficient units in the polymer structure becomes more electron-deficient, making the polymer molecules more easily p-doped, resulting in a narrower energy gap of the polymer and easier absorption of larger infrared light. The optical band gap of the polymer film was calculated by a reported method using the onset which was corresponding to the maximum absorption wavelength. The calculated optical band gap value was 0.79 eV.

The electrochromic results of the POTBTP film was shown in Fig. 8b. The POTBTP film was also yellow-green in the neutral state, and there was a wide absorption band between 600 nm and 1600 nm in the visible-near infrared region similar to the POTPTP film. When the applied potential gradually increased from 0 V to higher potential, the color of the polymer film faded, gradually changing from yellow-green to gray. This color change process indicates that the polymer is more prone to π-π * transition as the p-doping degree increases. As the oxidation potential increases from +0 V to +1.1 V, the absorption peak at 1011 nm of the polymer film was red-shifted, with a red shifting value about 556 nm, and eventually appeared at 1567 nm. The calculated optical band gap value was 0.79 eV which was calculated by the onset of the maximum absorption wavelength.

It is shown in Fig. 8 that the color change of the POTPTP film occurs within the voltage range from +0.6 V to +1.3 V, which is higher and narrower, while the electrochromism of POTBTP occurs within the voltage from 0 V to +1.1 V, which is lower and wider. The POTBTP has a higher electrochromic efficiency than POTPTP in the NIR region. The differences between POTPTP and POTBTP in the red shift of absorption bands (compared to the absorption spectrum of POTPTP film in neutral and oxidized states, the absorption spectrum of POTOP film were red- shifted about 16 nm and 180 nm, respectively), electrochromic voltage range and electrochromic efficiency are due to the difference in the structure of the electron-deficient unit in the polymer structure. The two pyridine rings in the electron deficient group of POTPTP have made the quinoxaline unit more electron-deficient and enhanced the electron- withdrawing capability, leaving the thiophene ring more electron-deficient thus demanding a higher applied potential for the oxidation and doping of the thiophene ring. Meanwhile, the thiophene ring was partially doped during electrochemical polymerization, thus the doping amount of POTPTP was small and this led to smaller red shift in the absorption band, together with higher and narrower electrical potential range. On the contrary, the thiophene rings in POTBTP are electron-rich and can easily be oxidized in a lower electrical potential, leading to doping with more counter

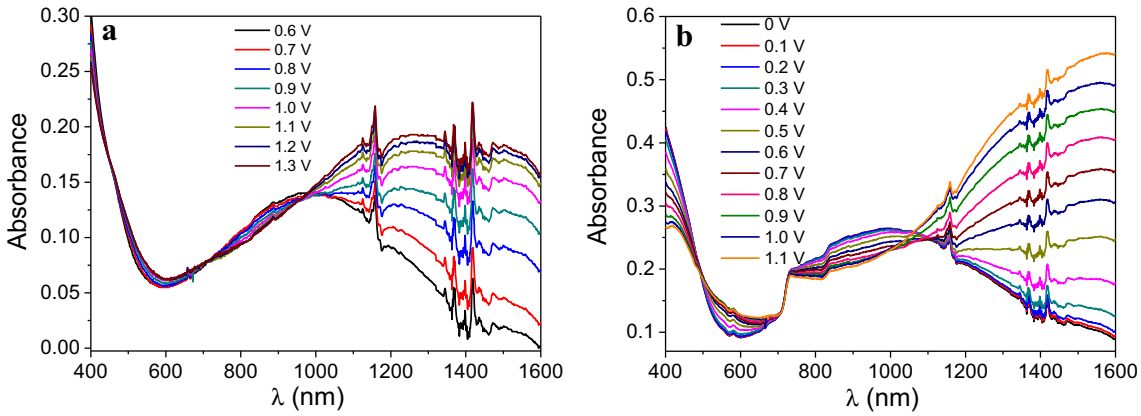

Fig. 8 p-Doping spectroelectrochemistry of (**a**) POTPTP film and (**b**) POTBTP film on an ITO coated glass slide in monomer free ACN/DCM (95:5) solution containing 0.1 M TBAPF6 electrolyte couple with applied potentials between 0.6 and + 1.3 V for POTTP, and between 0 and 1.1 V for POTBTP

ion than POTPTP which results in larger red shift in absorption band and higher electrochromic efficiency.

Electrochromic switching

In order to qualitatively and quantitatively analyze the stability, response time, and color conversion ability of the electrochemically polymerized polymer thin film during frequent and rapid transitions between the oxidized state and the reduced state, the polymer film which was fixed on the ITO glass surface was placed in an electrolyte solution, and the optical switching capability was examined via square wave potential step method combined with spectroscopy (Fig. 9). Before conducting the test, the wavelength and corresponding potential range to the maximum change in the transmittance was determined based on the absorption intensity spectra at different potentials obtained by the electrochromic experiment (Fig. 8). For polymer POTPTP films, the potential switching range was +0.6 V to +1.3 V; and for polymer POTBTP films, the potential switching range was determined to be 0 V to +1.1 V, and each switching time interval was 10s. The experimental results showed that, at the neutral state (when applied potential was +0.6 V) and the oxidized state (when applied the highest potential, that was +1.3 V) of the polymer POTPTP film, the transmittance change at a wavelength of 1294 nm was 19%, while the transmittance at the wavelength of 1567 nm was 30% (Fig. 9). It can also be seen from the test results that the color change time of polymer POTPTP film from the neutral state to the oxidized state or from the oxidized state to the neutral state were both 5 s. By the same test method, the change of the light transmittance of the polymer POTBTP film at the wavelength of 1567 nm was 51%, and the color change time was also calculated as 5 s.

Therefore, from the results of electrochromism, it can be concluded that the two low band gap polymer films of electrochemical polymerization have good color changing ability and stability in the NIR region.

Conclusions

To summarize, a Stille coupling reaction was applied to the synthesis of two D-A-D type quinoxline monomers, OTPTP and OTBTP, and the electrochromic properties of their polymer films which were synthesized on the ITO glass surface by electrochemical polymerization were studied. The electronic characteristics of two different electron-withdrawing groups and their influences on the electrochemical polymerization

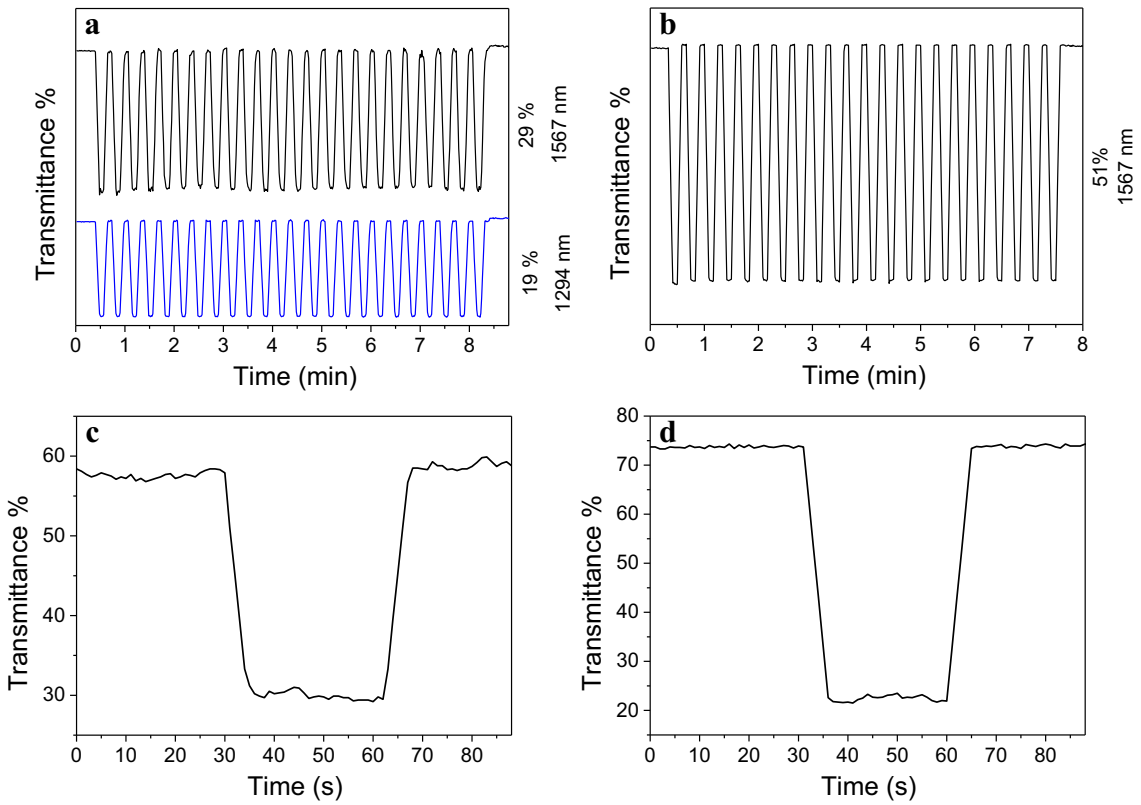

Fig. 9 Electrochromic switching, optical absorbance change monitored of at (**a**) 1294 nm and 1567 nm for POTPTP and (**b**) 1567 nm for POTBTP; Electrochromic switching stability of POTPTP (**c**) and of POTBTP (**d**)

of monomers and electrochromic performance of the obtained polymers were observed. The electronic performance of monomers illustrated that OTBTP can be polymerized in the lower potential range than OTPTP due to the stronger electron-withdrawing capability of the electron-withdrawing groups in OTPTP which contains two dipyridine unit. The UV Visible NIR spectra analysis showed that both polymers, POTPTP and POTBTP, have one broad absorbance band in the region of 400 ~ 1600 nm at the neutral state, and spectroelectrochemical spectra showed that both POTPTP and POTBTP possess good color changing ability in NIR region via easily accessible p-type doping. The experimental results showed that the transmittance change of polymer POTPTP film at a wavelength of 1294 nm was 19%, while the transmittance at the wavelength of 1567 nm was 30%. The change of the light transmittance of the polymer POTBTP film at the wavelength of 1567 nm was 51%. The electrochromic analysis revealed that the two polymer films exhibited reasonable optical contrasts in the infrared region of 1000 ~ 1600 nm with low response time (about 5 s) and low band gap.

Acknowledgements This work was financially supported by the National Natural Science Foundation of China (No. 21662034) and Doctoral Initiation Fund of Xinjiang University (No.BS150226 and No. BS180218). We sincerely appreciate the support.

References

1. Lee JY, Han S-Y, Lim B, Nah Y-C (2019) A novel quinoxaline-based donor-acceptor type electrochromic polymer. J Ind Eng Chem 70:380–384. https://doi.org/10.1016/j.jiec.2018.10.039
2. Bhadra J, Alkareem A, Al-Thani N (2020) A review of advances in the preparation and application of polyaniline based thermoset blends and composites. J Polym Res 27(5):122. https://doi.org/10.1007/s10965-020-02052-1
3. Jiramitmongkon K, Chotsuwan C, Asawapirom U, Hirunsit P (2020) Cyclopentadithiophene and Diketo-pyrrolo-pyrrole fused rigid copolymer for high optical contrast electrochromic polymer. J Polym Res 27(1):17. https://doi.org/10.1007/s10965-019-1989-9
4. Chen X, Zhang J (2020) Blue-to-transmissive electrochromic poly(2,3-dimethyl-2,3-dihydrothieno[3,4-b][1,4]dioxine) (PEDOT-Me2) with improved optical contrast. J Solid State Electrochem 24(2):441–445. https://doi.org/10.1007/s10008-019-04343-0
5. Kim HN, Cho SM, Ah CS, Song J, Ryu H, Kim YH, Kim T-Y (2016) Electrochromic mirror using viologen-anchored nanoparticles. Mater Res Bull 82:16–21. https://doi.org/10.1016/j.materresbull.2016.03.010
6. Li S, Wang X, Hu R, Chen H, Li M, Wang J, Wang Y, Liu L, Lv F, Liang X-J, Wang S (2016) Near-infrared (NIR)-absorbing conjugated polymer dots as highly effective Photothermal materials for in vivo Cancer therapy. Chem Mater 28(23):8669–8675. https://doi.org/10.1021/acs.chemmater.6b03738
7. Liu S, Chen C, Li Y, Zhang H, Liu U, Wong S, Lam JWY, Ding D, Tang BZ (2019) Constitutional Isomerization Enables Ultrabright NIR-II AIEgen for Brain-Inflammation Imaging. *Adv Funct Mater* *30*(7):1908125. https://doi.org/10.26434/chemrxiv.8684693.v1
8. Okamoto Y, Tanioka M, Muranaka A, Miyamoto K, Aoyama T, Ouyang X, Kamino S, Sawada D, Uchiyama M (2018) Stable Thiele's hydrocarbon derivatives exhibiting near-infrared absorption/emission and two-step Electrochromism. J Am Chem Soc 140(51):17857–17861. https://doi.org/10.1021/jacs.8b11092
9. Wang B, Yuan H, Liu Z, Nie C, Liu L, Lv F, Wang Y, Wang S (2014) Cationic Oligo(p-phenylene vinylene) materials for combating drug resistance of Cancer cells by light manipulation. Adv Mater 26(34):5986–5990. https://doi.org/10.1002/adma.201402183
10. Dong H, Zhu H, Meng Q, Gong X, Hu W (2012) Organic photoresponse materials and devices. Chem Soc Rev 41(5):1754–1808. https://doi.org/10.1039/c1cs15205j
11. Maiorov VA (2019) Electrochromic glasses with separate regulation of transmission of visible light and near-infrared radiation (review). Opt Spectrosc 126(4):412–430. https://doi.org/10.1134/s0030400x19040143
12. Żmija J, Małachowski MJ (2011) New organic electrochromic materials and theirs applications. J Achiev Mater Manuf Eng 48(1):14–23
13. Kline WM, Lorenzini RG, Sotzing GA (2014) A review of organic electrochromic fabric devices. Color Technol 130(2):73–80. https://doi.org/10.1118/1.2167371
14. Zhang W, Zhu C, Huang Z, Gong C, Tang Q, Fu X (2019) Electrochromic 2,4,6-triphenyl-1,3,5-triazine based esters with electron donor-acceptor structure. Org Electron 67:302–310. https://doi.org/10.1016/j.orgel.2018.12.041
15. Ozyurt F, Durmus A, Gorkem Gunbas E, Toppare L (2010) A low-band gap conductive copolymer of bis-3-hexylthiophene substituted 4-tert-butylphenyl quinoxaline and 3,4-ethylenedioxythiophene. J Solid State Electrochem 14(2):279–283. https://doi.org/10.1007/s10008-008-0750-9
16. Pamuk M, Tirkeş S, Cihaner A, Algı F (2010) A new low-voltage-driven polymeric electrochromic. Polymer 51(1):62–68. https://doi.org/10.1016/j.polymer.2009.11.009
17. Esmer EN, Tarkuc S, Udum YA, Toppare L (2011) Near infrared electrochromic polymers based on phenazine moieties. Mater Chem and Phys 131(1–2):519–524. https://doi.org/10.1016/j.matchemphys.2011.10.014
18. Carbas BB, Kivrak A, Zora M, Önal AM (2012) Synthesis and electropolymerization of a new ion sensitive ethylenedioxy-substituted terthiophene monomer bearing a quinoxaline moiety. J Electroanal Chem 677-680:9–14. https://doi.org/10.1016/j.jelechem.2012.05.005
19. Cevher SC, Hizalan G, Temiz C, Udum YA, Toppare L, Cirpan A (2016) Effect of substituent groups on quinoxaline-based random copolymers on the optoelectronic and photovoltaic properties. Polymer 101:208–216. https://doi.org/10.1016/j.polymer.2016.08.076
20. Suganya S, Kim N, Jeong JY, Park JS (2017) Benzotriazole-based donor-acceptor type low band gap polymers with a siloxane-terminated side-chain for electrochromic applications. Polymer 116:226–232. https://doi.org/10.1016/j.polymer.2017.03.075
21. BaluAtar A, YunJeong J, HunHanJong S, Park S (2018) Efficient blue-to-transmissive electrochromic transitions of alkylated quinoxaline-thiophene based donor-acceptor type conjugated polymers. Polymer 153:95–102. https://doi.org/10.1016/j.polymer.2018.08.009
22. Mahmut M, Awut T, Nurulla I, Mijit M (2014) Synthesis and spectroelectrochemical investigation of low-bandgap polymer: integrated quinoxaline and benzimidazole in one electron acceptor unit. J Appl Polym Sci 131(19):40861. https://doi.org/10.1002/app.40861
23. Mahmut M, Awut T, Nurulla I, Mijit M (2014) Synthesis of two novel acenaphthyl-quinoxaline based low-band gap polymers and

its electrochromic properties. J Polym Res 21(4):403. https://doi.org/10.1007/s10965-014-0403-x
24. Mahmut M, Awut T, Nurulla I (2015) Low band gap polymers synthesized by electrochemical polymerization for electrochromic devices. Chinese J Polym Sci 33(10):1442–1452. https://doi.org/10.1007/s10118-015-1698-8
25. Tarkuc S, Unver EK, Udum YA, Toppare L (2010) Multi-colored electrochromic polymer with enhanced optical contrast. Eur Polym J 46(11):2199–2205. https://doi.org/10.1016/j.eurpolymj.2010.08.002
26. Guo W, Engelman BJ, Haywood TL, Blok NB, Beaudoin DS, Obare SO (2011) Dual fluorescence and electrochemical detection of the organophosphorus pesticides—Ethion, malathion and fenthion. Talanta 87:276–283. https://doi.org/10.1016/j.talanta.2011.10.015
27. Ergang Wang LH, Wang Z, Hellström S, Mammo W, Zhang F, Inganäs O, Andersson MR (2010) Small Band Gap Polymers Synthesized via a Modified Nitration of 4,7-Dibromo-2,1,3-benzothiadiazole. *Org Lett 12*(20):4470–4473. https://doi.org/10.1021/ol1020724
28. Cai T, Zhou Y, Wang E, Hellström S, Zhang F, Xu S, Inganäs O, Andersson MR (2010) Low bandgap polymers synthesized by FeCl3 oxidative polymerization. *Sol Energy Mater Sol Cells 94*: 1275–1281. https://doi.org/10.1016/j.solmat.2010.03.024
29. Zhang Y, Shi J, He X, Tu G (2016) All-thiophene-substituted N-heteroacene electron-donor materials for efficient organic solar cells. J Mater Chem A 4(35):13519–13524. https://doi.org/10.1039/c6ta03784d
30. Perzon E, Wang X, Admassie S, Ingana O, Anderson MR (2006) An alternating low band-gap polyfluorene for optoelectronic devices. Polymer 47:4261–4268. https://doi.org/10.1016/j.polymer.2006.03.110
31. Zhou S, An C, Stelzig T, Puniredd SR, Guo X, Pisula W, Baumgarten M (2015) Strengthening the acceptor properties of thiadiazoloquinoxalines via planarization. New J Chem 39(9): 6765–6770. https://doi.org/10.1039/c5nj00517e
32. Yuen JD, Fan J, Seifter J, Lim B, Hufschmid R, Heeger AJ, Wudl F (2011) High performance weak donor–acceptor polymers in thin film transistors: effect of the acceptor on electronic properties, Ambipolar conductivity, mobility, and thermal stability. J Am Chem Soc 133(51):20799–20807. https://doi.org/10.1021/ja205566w
33. Baran D, Balan A, Celebi S, Meana Esteban B, Neugebauer H, Sariciftci NS, Toppare L (2010) Processable multipurpose conjugated polymer for Electrochromic and photovoltaic applications. Chem Mater 22(9):2978–2987. https://doi.org/10.1021/cm100372t
34. Eva Bundgaard FCK (2006) Low-band-gap conjugated polymers based on Thiophene, Benzothiadiazole, and Benzobis(thiadiazole). *Macromolecules 39*(8):2823–2831. https://doi.org/10.1021/ma052683e
35. Sun Y, Zhu G, Zhao X, Kang W, Li M, Zhang X, Yang H, Guo L, Lin B (2020) Solution-processable, hypercrosslinked polymer via post-crosslinking for electrochromic supercapacitor with outstanding electrochemical stability. Sol Energy Mater Sol Cells 215: 110661. https://doi.org/10.1016/j.solmat.2020.110661
36. Yang S, Sun B, Liu Y, Zhu J, Song J, Hao Z, Zeng X, Zhao X, Shu Y, Chen J, Yi J, He J (2020) Effect of ITO target crystallinity on the properties of sputtering deposited ITO films. Ceram Int 46(5): 6342–6350. https://doi.org/10.1016/j.ceramint.2019.11.110
37. Tamilavan V, Lee J, Kwon JH, Jang S, Shin I, Agneeswari R, Jung JH, Jin Y, Park SH (2019) Side-chain influences on the properties of benzodithiophene-alt-di(thiophen-2-yl)quinoxaline polymers for fullerene-free organic solar cells. Polymer 172:305–311. https://doi.org/10.1016/j.polymer.2019.04.011